Machining Science and Technology
Publication details, including instructions for authors and subscription information:
http://www.informaworld.com/smpp/title~content=t713597283

ON STABILITY PREDICTION FOR LOW RADIAL IMMERSION MILLING

J. Gradišek[a]; E. Govekar[a]; I. Grabec[a]; M. Kalveram[b]; K. Weinert[b]; T. Insperger[c]; G. Stépán[c]
[a] Faculty of Mechanical Engineering, University of Ljubljana, Slovenia [b] Department of Machining Technology (ISF), University of Dortmund, Germany [c] Department of Applied Mechanics, Budapest University of Technology and Economics, Hungary

To cite this Article Gradišek, J. , Govekar, E. , Grabec, I. , Kalveram, M. , Weinert, K. , Insperger, T. and Stépán, G.(2005) 'ON STABILITY PREDICTION FOR LOW RADIAL IMMERSION MILLING', Machining Science and Technology, 9: 1, 117 — 130
To link to this Article: DOI: 10.1081/MST-200051378
URL: http://dx.doi.org/10.1081/MST-200051378

Machine Science and Technology, 9:117–130

ISSN: 1091-0344 print/1532-2483 online
DOI: 10.1081/MST-200051378

Taylor & Francis
Taylor & Francis Group

ON STABILITY PREDICTION FOR LOW RADIAL IMMERSION MILLING

J. Gradišek, E. Govekar, and I. Grabec □ *Faculty of Mechanical Engineering, University of Ljubljana, Slovenia*

M. Kalveram and K. Weinert □ *Department of Machining Technology (ISF), University of Dortmund, Germany*

T. Insperger and G. Stépán □ *Department of Applied Mechanics, Budapest University of Technology and Economics, Hungary*

□ *Stability boundaries for milling are predicted by the zeroth-order approximation (ZOA) and the semi-discretization (SD) methods. For high radial immersions, the methods predict similar stability boundaries. As radial immersion is decreased, the disagreement between the predictions of the two methods grows considerably. The most prominent difference is an additional type of instability predicted only by the SD method. The experiments confirm the predictions of the SD method. Three different types of tool motion are observed: periodic chatter-free, quasiperiodic chatter, and periodic chatter motion. Tool displacements recorded during each of the three motion types are analyzed.*

Keywords End Milling, Stability Prediction

INTRODUCTION

High material removal rates, provided in theory by the modern machining centers, often can not be achieved in practice due to the inherent instability of a cutting process. In cutting processes that involve rotation of the tool or workpiece, the instability is caused by the so called regeneration of surface waviness during successive cuts. The instability is called regenerative chatter.

Dynamics of regenerative cutting processes can be described by models in the form of linear delay-differential equations (DDEs) (1, 2). Chatter-free cutting and chatter correspond to the linearly stable and unstable solutions of the model equations, respectively. Cutting parameters that assure

Address correspondence to J. Gradišek, Faculty of Mechanical Engineering, University of Ljubljana, Aškerčeva 6, Ljubljana, SI-1000, Slovenia. E-mail: janez.gradisek@fs.uni-lj.si

stable, chatter-free, machining can therefore be predicted by the linear stability analysis of the equations. For continuous cutting, such as uninterrupted turning, the stability boundary can be given in closed form while for interrupted machining, such as milling and interrupted turning, the periodic dependence of the cutting force complicates the stability analysis so that the stability boundary in general cannot be given in closed form.

The first analytical attempts at stability prediction of milling were based on Fourier expansion of the periodic cutting forces (3). Accuracy of the obtained stability boundary depends on the shape of cutting force variation and the number of Fourier terms used to approximate it. For cutters with a large number of teeth and for substantial radial immersions, reasonably accurate stability predictions can be achieved by using only the zeroth-order Fourier term (4, 5). However, for cutters with few teeth and for low radial immersions, prohibitively many Fourier coefficients may be needed to capture the cutting force variation. In such cases, which are quite common in high-speed milling, the exact stability boundary may differ significantly from the one predicted by the zeroth-order approximation (ZOA) (6).

This was first shown for the case of very low immersion milling, where the time interval of the tool-workpiece contact was a small fraction of the tool revolution period (6). Using an impact-like representation of the cutting process, a new method for stability prediction was derived that revealed that there are two types of instability possible in low immersion milling: the Hopf bifurcation, which causes the quasiperiodic chatter, and the period doubling or flip bifurcation, which causes the periodic chatter. In contrast, the ZOA predicts only one type of instability, the Hopf bifurcation.

The stability predictions from (6) lose accuracy as the time of the tool-workpiece contact increases. Two alternative methods have since been proposed that can predict stability boundary for an arbitrary time in the cut (7). The first method combines the exact analytical solution of the free tool vibration with the approximate solution for the tool vibration during cutting which is calculated using temporal finite element analysis (TFEA). The second method employs a semi-discretization (SD) scheme to transform the DDE into a series of autonomous ordinary differential equations (ODEs) for which the solutions are known. Both methods define a transition matrix whose eigenvalues determine stability of the process. The methods have been derived and verified experimentally using a 1-dof milling system (8). Recently, the TFEA method has been extended to 2-dof systems (9).

In this paper, the stability of a 2-dof milling system is investigated. Stability boundaries are predicted using the ZOA and the SD methods; the latter is also adapted for a 2-dof system. Stability predictions of the two methods are compared and verified experimentally on a high speed milling center. The recorded tool paths in the X-Y plane are analyzed and three different

types of tool motion predicted by the SD method are distinguished: periodic chatter-free, quasiperiodic, and periodic chatter motion.

STABILITY PREDICTION FOR END MILLING

Consider a 2-dof milling operation shown schematically in Figure 1. A cutter with N equally spaced teeth rotates at a constant angular velocity Ω. The radial immersion angle of the jth tooth varies with time as: $\phi_j(t) = \Omega t + 2\pi(j-1)/N$. A compliant machine tool structure is excited by the cutting forces at the tool tip, causing dynamic response of the structure governed by the following equation:

$$\mathbf{M}\ddot{\mathbf{X}}(t) + \mathbf{C}\dot{\mathbf{X}}(t) + \mathbf{K}\mathbf{X}(t) = \mathbf{F}(t) \tag{1}$$

Here $\mathbf{X}$ and $\mathbf{F}$ denote the displacement and cutting force vectors, while $\mathbf{M}$, $\mathbf{C}$, and $\mathbf{K}$ denote the mass, damping and stiffness matrices, which are all diagonal if the vibration modes in X and Y directions are uncoupled. Dimensionality of the vectors and matrices depends on the number of vibration modes. Assuming a single vibration mode in X and Y directions, the vectors are 2×1 and the matrices 2×2 dimensional. The cutting force components acting on the jth tooth are given by:

$$\begin{aligned} F_{x,j} &= g_j(t)\Big(-F_{\mathrm{t},j}(t)\cos\phi_j(t) - F_{\mathrm{r},j}(t)\sin\phi_j(t)\Big) \\ F_{y,j} &= g_j(t)\Big(+F_{\mathrm{t},j}(t)\sin\phi_j(t) - F_{\mathrm{r},j}(t)\cos\phi_j(t)\Big) \end{aligned} \tag{2}$$

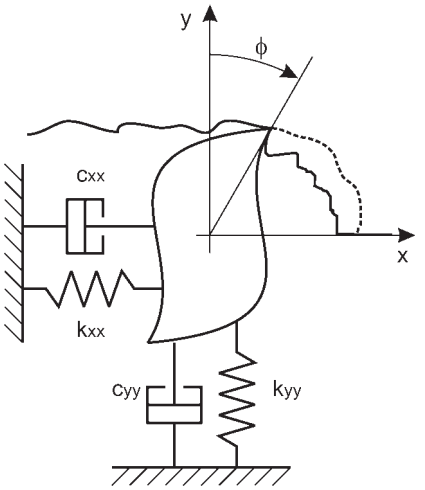

FIGURE 1 Scheme of 2-dof milling.

Here, $g_j(t)$ is a unit step function determining whether or not the jth tooth is cutting. The tangential and radial cutting force components, F_t and F_r, are assumed proportional to the chip load defined by the product of chip thickness $h_j(t)$ and chip width or depth of cut a_p as:

$$F_{t,j}(t) = K_t a_p h_j(t), \quad F_{r,j}(t) = k_r F_{t,j}(t) \tag{3}$$

K_t and k_r, respectively, denote the specific tangential force coefficient and the force ratio. The chip thickness consists of a static part due to feed, $s_t \sin\phi(t)$, and a dynamic part due to cutter displacement. The stability of cutting is influenced only by the dynamic part of chip thickness given by:

$$h_j(t) = g_j(t)\Big(\Delta x \sin\phi_j(t) + \Delta y \cos\phi_j(t)\Big) \tag{4}$$

where $\Delta x = x(t) - x(t-T)$ and $\Delta y = y(t) - y(t-T)$ describe the surface regeneration, i.e. the difference between the tool positions at the present and previous tooth passes. $T = 2\pi/N\Omega$ denotes the tooth passing period.

Summing the contributions of all cutting edges yields the total cutting force:

$$\begin{bmatrix} F_x(t) \\ F_y(t) \end{bmatrix} = a_p K_t \begin{bmatrix} A_{xx}(t) A_{xy}(t) \\ A_{yx}(t) A_{yy}(t) \end{bmatrix} \cdot \begin{bmatrix} \Delta x(t, T) \\ \Delta y(t, T) \end{bmatrix} \tag{5}$$

where $A_{ij}(t)$ denote the time periodic directional dynamic force coefficients:

$$\begin{aligned}
A_{xx}(t) &= \frac{1}{2}\sum_{j=1}^{N}\Big(-\sin 2\phi_j(t) - 2k_r \sin^2\phi_j(t)\Big) g_j(t) \\
A_{xy}(t) &= \frac{1}{2}\sum_{j=1}^{N}\Big(-2\cos^2\phi_j(t) - k_r \sin 2\phi_j(t)\Big) g_j(t) \\
A_{yx}(t) &= \frac{1}{2}\sum_{j=1}^{N}\Big(+2\sin^2\phi_j(t) - k_r \sin 2\phi_j(t)\Big) g_j(t) \\
A_{yy}(t) &= \frac{1}{2}\sum_{j=1}^{N}\Big(+\sin 2\phi_j(t) - 2k_r \cos^2\phi_j(t)\Big) g_j(t)
\end{aligned} \tag{6}$$

Finally, the governing delay differential equation (DDE) of motion reads:

$$\mathbf{M}\ddot{\mathbf{X}}(t) + \mathbf{C}\dot{\mathbf{X}}(t) + \mathbf{K}\mathbf{X}(t) = a_p K_t \boldsymbol{A}(t)(\mathbf{X}(t) - \mathbf{X}(t-T)) \tag{7}$$

Time dependence of the directional coefficients $A_{ij}(t)$ complicates the linear stability analysis of Equation (7). A possible solution to this problem

is to expand the coefficients in a Fourier series and retain the terms necessary for the approximation. In the simplest case, which is briefly reviewed below, only the zeroth-order Fourier term is kept. Such an approximation is practical as it allows a closed-form expression of the stability boundary, but it loses accuracy as the radial immersion and the number of cutter teeth decrease. Another possibility is the recently proposed time domain methods, the temporal finite element analysis (TFEA) or the semi-discretization method (7). The latter is presented in Section 2.2.

Zeroth-Order Approximation Method

The zeroth-order approximation method was proposed in Reference (5). It is based on approximating the periodic directional milling force coefficient by its average value, $\mathbf{A}(t) \approx \mathbf{A}_0$. The resulting approximate milling force vector is:

$$\mathbf{F}(t) = a_p K_t \mathbf{A}_0 (\mathbf{X}(t) - \mathbf{X}(t - T)) \tag{8}$$

The cutter displacement $\mathbf{X}$ caused by the force $\mathbf{F}$ can be expressed by means of a transfer function $\mathbf{H}$ of the machine tool structure in the Laplace domain as:

$$\begin{bmatrix} X(s) \\ Y(s) \end{bmatrix} = \begin{bmatrix} H_{xx}(s) H_{xy}(s) \\ H_{yx}(s) H_{yy}(s) \end{bmatrix} \cdot \begin{bmatrix} F_x(s) \\ F_y(s) \end{bmatrix} \tag{9}$$

By combining Equations (8) and (9), a system of equations is obtained:

$$[\mathbf{I} + \Lambda(s) \mathbf{A}_0 \mathbf{H}(s)] \mathbf{F}(s) = \mathbf{0} \tag{10}$$

where $\Lambda(s) = -a_p K_t (1 - \exp(-sT))$ and $\mathbf{I}$ denotes the identity matrix. The system has a nontrivial solution only if its determinant is zero:

$$\det[\mathbf{I} + \Lambda(s) \mathbf{A}_0 \mathbf{H}(s)] = 0 \tag{11}$$

Signs of the real part of the roots of Equation (11) determine stability of the system. On the stability boundary, the real part is zero, so that $s = j\omega_c$, where ω_c denotes the chatter frequency. By a substitution of $s = j\omega_c$ into Equation (11), a quadratic equation for Λ is obtained from which the values of the cutting depth a_p and chatter frequency ω_c at the stability boundary can be calculated. Further details on this procedure can be found in References (4) and (5).

It should be pointed out that there exist two solutions of the quadratic equation for Λ, which yield different stability boundaries. The procedure itself does not indicate which of the two solutions is correct. According

to the experience of the authors, one of the boundaries has usually, but not always, unrealistically high values of the cutting depth that distinguishes it from the correct boundary. Some caution is therefore required in the final steps of the procedure.

Semi-Discretization Method

The basic idea of the semi-discretization (SD) method is to approximate the delayed terms of the DDE by a piecewise constant function while leaving the current time terms unchanged. This way, the DDE is approximated by a series of ODEs for which the solutions can be given in closed form.

In the case of 2-dof milling, the Equation (7) may be rewritten as:

$$\mathbf{M}\ddot{\mathbf{X}}(t) + \mathbf{C}\dot{\mathbf{X}}(t) + (\mathbf{K} + \mathbf{Q}(t))\mathbf{X}(t) = \mathbf{Q}(t)\mathbf{X}(t - T) \tag{12}$$

where $\mathbf{Q}(t) = -a_{\mathrm{p}}K_{\mathrm{t}}\mathbf{A}(t)$ was used to simplify the notation. Discretization is introduced using a time interval $\Delta t = \left[t_i, t_{i+1}\right)$. The delay time becomes $T = (m + 0.5)\Delta t$, where m is an integer determining the coarseness of the discretization. The periodic coefficient $\mathbf{Q}(t) = \mathbf{Q}(t + T)$ and the delayed state $\mathbf{X}(t - T)$ are approximated by:

$$\begin{aligned}&\mathbf{Q}(t) \approx \mathbf{Q}(t_i) = \mathbf{Q}_i\\ &\mathbf{X}(t - T) \approx 0.5(\mathbf{X}(t_{i-m+1}) + \mathbf{X}(t_{i-m})) = 0.5(\mathbf{X}_{i-m+1} + \mathbf{X}_{i-m}).\end{aligned} \tag{13}$$

The DDE in Equation (12) is herewith transformed into a series of autonomous second order ODEs:

$$\mathbf{M}\ddot{\mathbf{X}}(t) + \mathbf{C}\dot{\mathbf{X}}(t) + (\mathbf{K} + \mathbf{Q}_i)\mathbf{X}(t) = \frac{\mathbf{Q}_i}{2}(\mathbf{X}_{i-m+1} + \mathbf{X}_{i-m}), \tag{14}$$

which can be rewritten as systems of first order ODEs:

$$\dot{\mathbf{u}}(t) = \mathbf{W}_i\mathbf{u}(t) + \mathbf{V}_i(\mathbf{u}_{i-m+1} + \mathbf{u}_{i-m}) = \mathbf{W}_i\mathbf{u}(t) + \mathbf{w}_i \tag{15}$$

with $\mathbf{u} = [\dot{x}, \dot{y}, x, y]$. For the initial condition $\mathbf{u}(t_i) = \mathbf{u}_i$, the solution of Eq. (15) is:

$$\mathbf{u}(t) = \exp(\mathbf{W}_i(t - t_i))\left(\mathbf{u}_i + \mathbf{W}_i^{-1}\mathbf{w}_i\right) - \mathbf{W}_i^{-1}\mathbf{w}_i. \tag{16}$$

Substituting $t = t_{j+1}$ and $\mathbf{u}\left(t_{j+1}\right) = \mathbf{u}_i$ into this solution gives:

$$\begin{aligned}\mathbf{u}_{i+1} &= \exp(\mathbf{W}_i\Delta t)\mathbf{u}_i + (\exp(\mathbf{W}_i\Delta t) - \mathbf{I})\mathbf{W}_i^{-1}\mathbf{V}_i(\mathbf{u}_{i-m+1} + \mathbf{u}_{i-m})\\ &= \mathbf{P}_i\mathbf{u}_i + \mathbf{R}_i(\mathbf{u}_{i-m+1} + \mathbf{u}_{i-m})\end{aligned} \tag{17}$$

Eq. (17) can be recast into a map

$$\mathbf{v}_{i+1} = \mathbf{Z}_i \mathbf{v}_i \tag{18}$$

with the state vector $\mathbf{v}_i = [\mathbf{u}_i,\ \mathbf{u}_{i-1},\ \ldots, \mathbf{u}_{i-m}]$ and the coefficient matrix:

$$\mathbf{Z}_i = \begin{bmatrix} \mathbf{P}_i & \mathbf{0} & \mathbf{0} & \ldots & \mathbf{0} & \mathbf{R}_i & \mathbf{R}_i \\ \mathbf{I} & \mathbf{0} & \mathbf{0} & \ldots & \mathbf{0} & \mathbf{0} & \mathbf{0} \\ \mathbf{0} & \mathbf{I} & \mathbf{0} & \ldots & \mathbf{0} & \mathbf{0} & \mathbf{0} \\ \vdots & \vdots & \vdots & \ddots & \vdots & \vdots & \vdots \\ \mathbf{0} & \mathbf{0} & \mathbf{0} & \ldots & \mathbf{I} & \mathbf{0} & \mathbf{0} \\ \mathbf{0} & \mathbf{0} & \mathbf{0} & \ldots & \mathbf{0} & \mathbf{I} & \mathbf{0} \end{bmatrix} \tag{19}$$

The Floquet transition matrix over the principal period T is approximated by coupling the solution of m successive intervals as:

$$\mathbf{\Phi} = \mathbf{Z}_{m-1}\mathbf{Z}_{m-2}\cdots\mathbf{Z}_1\mathbf{Z}_0 \tag{20}$$

Stability of the investigated system is determined by the eigenvalues of the transition matrix (10). The system is stable if all eigenvalues of $\mathbf{\Phi}$ are in modulus less than 1.

Two possible instabilities can be observed in the case of milling. First, the eigenvalue of $\mathbf{\Phi}$ is complex and its modulus is greater than 1. This case corresponds to the Hopf bifurcation causing the quasiperiodic chatter. Second, the eigenvalue is real and its value is smaller than -1. This case corresponds to the period doubling or flip bifurcation, which causes the periodic chatter. Further details on the semi-discretization procedure can be found in Reference (7).

EXPERIMENTAL RESULTS

The cutting tests were conducted on a high-speed milling center with a cylindrical end mill with a single cutting edge, 8 mm diameter, 45 degree helix angle, and 96 mm overhang ($L/D = 12$). Originally, the cutter had two teeth, but one tooth was removed in order to avoid disturbances due to the outrun. The cutter was mounted in a HSK40E shrinkfit holder. The workpiece material was AlMgSi0.5 aluminum alloy for which the specific tangential force coefficient and the force ratio were determined mechanistically (11): $K_t = 644$ MPa and $k_r = 0.37$.

The tool deflections during cutting were measured in X and Y directions simultaneously by a couple of laser-optical displacement sensors mounted on the spindle housing. The sampling rate of the sensors was 10 kHz. The measurement point on the tool shaft was located 63 mm above the tool tip.

A photo diode was attached to the spindle housing in order to detect black/white transition painted on the rotating tool holder. The transition occurred once per tool revolution, giving a signal synchronized with the spindle rotation. The signal was used for off-line stroboscope resampling of the displacements records.

Modal Analysis

The transfer function matrix **H** of the machine tool structure was determined by a standard impact test procedure. For the stability prediction, the transfer function at the tool tip is required. However, due to the flexible tool of a small diameter the excitation at the tool tip using an instrumented hammer with a 100 g head was not impulse-like. Regular excitation could only be assured by hitting the tool shaft below the tool holder. Consequently, the transfer function at the tool tip could not be measured directly; instead, it had to be calculated from the measurements at the excitation point located 15 mm below the tool holder.

To facilitate such a calculation, the tool response in X and Y directions was measured by two pairs of low mass accelerometers attached to the tool at the excitation point and at the tool tip. The transfer functions at the excitation point, obtained by averaging 10 responses, were curve fit using commercial modal analysis software to determine the modal parameters and the modal matrix, from which the transfer functions at the tool tip were calculated. The resulting modal parameters at the tool tip are listed in Table 1.

Due to the large tool overhang, the transfer function of the machine tool structure is dominated by a single vibration mode at $f_t \approx 720$ Hz, which corresponds to the tool's first bending mode. The frequencies of the mode in X and Y directions are slightly different. The out-of-diagonal (xy and yx) matrix elements, which would indicate the presence of coupling between the modes in X and Y directions, were much smaller than the diagonal (xx and yy) elements and their calculation was quite unreliable. Consequently, the out-of-diagonal elements were set to zero making the transfer function matrix diagonal, which means that the potential mode coupling was neglected.

TABLE 1 Modal Parameters of the Cutter

	xx	yy
Mass [g]	20.1	19.9
Damping [kg/s]	1.56	1.60
Stiffness [kN/m]	414	409

xx and yy denote the indices of matrix elements.

Predicted Stability Charts

Stability charts were predicted by the zeroth-order approximation (ZOA) and semi-discretization (SD) methods for a series of radial depths of cut a_e. Charts for up-milling with $a_e = 0.5D,\ 0.25D$, and $0.05D$ are compared in Figure 2. For $a_e = 0.5D$ (50% radial immersion), both methods yield similar results: lobed stability boundaries with lobe maxima located at the integer fractions of the structure's dominant eigenfrequency, f_t/k. As radial depth of cut decreases, the discrepancy between the ZOA and SD stability boundaries grows considerably. The most prominent difference is the additional set of lobes located at the odd integer fractions of twice the dominant eigenfrequency, $2f_t/(2k+1)$. These lobes are predicted only by the SD method and correspond to the period doubling (flip) bifurcation which causes periodic chatter. They appear already at a full immersion cut ($a_e = D$, not shown) and grow steadily with decreasing radial immersion.

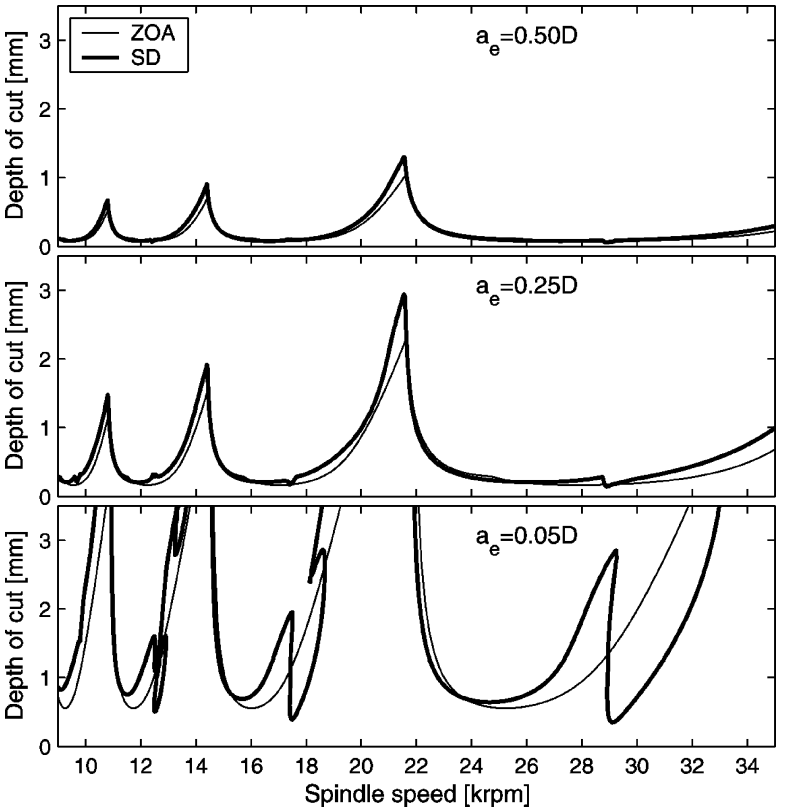

FIGURE 2 Stability charts predicted by the ZOA and SD methods.

The SD stability chart at $a_e = 0.05D$ reveals an intriguing structure; the flip lobe at $n = 12.5$ krpm is a closed curve within the stable domain, the lobe at $n = 18$ krpm is almost closed, and there are further lobe-like portions of the stability boundary at higher depths of cut (not shown). Similar structure of the stability chart was observed for a simulated 1-dof interrupted turning in (12), where it was proven rigorously that all flip lobes, except for the first one, are in fact closed curves distributed not only along the spindle speed axis but also across the entire $n-a_p$ plane. The stability chart for $a_e = 0.05D$ indicates that this property might also hold for realistic 2-dof milling systems.

Experimental Stability Charts

The predicted stability charts were verified experimentally by cutting tests conducted at a series of spindle speeds and cutting depths. Stability of cutting was assessed from the sound emitted during machining and from the recorded tool displacements. The results for the three radial immersions are summarized in Figure 3.

For $a_e = 0.5D$, the predictions and experiments agree very well. The observed stability maxima match the predicted ones along the entire spindle speed range, whereas the minima slightly increase as spindle speed is increased. This increase of stability could be attributed to decrease of cutting force coefficients at higher cutting speeds. At $n = 29$ krpm, a flip lobe was observed. Its location was correctly predicted by the SD method. For $a_e = 0.25D$, the agreement between predictions and experiments is still quite good. Notable discrepancies are observed mainly at the stability maxima, which are overestimated by both methods. The reason for this discrepancy is at present unknown. The flip lobes are observed close to the locations predicted by the SD method. The situation is similar for $a_e = 0.05D$, where the predicted structure of the stability chart is correct, but the stability maxima are significantly overestimated. Location of the flip lobes is predicted well, except for the lobe at $n = 28$ krpm which was found at lower spindle speeds than predicted.

Comparison of the Hopf and flip bifurcation lobes shows that the Hopf lobes are much wider than the flip ones whereas the latter often reach to lower depths of cut than the former. Since the Hopf and flip lobes are also located at different spindle speeds, it is important to consider both of them when selecting chatter-free cutting parameters.

TOOL PATHS IN X-Y PLANE

Three different types of tool motion corresponding to three different cutting regimes were predicted by the SD method and observed experimentally

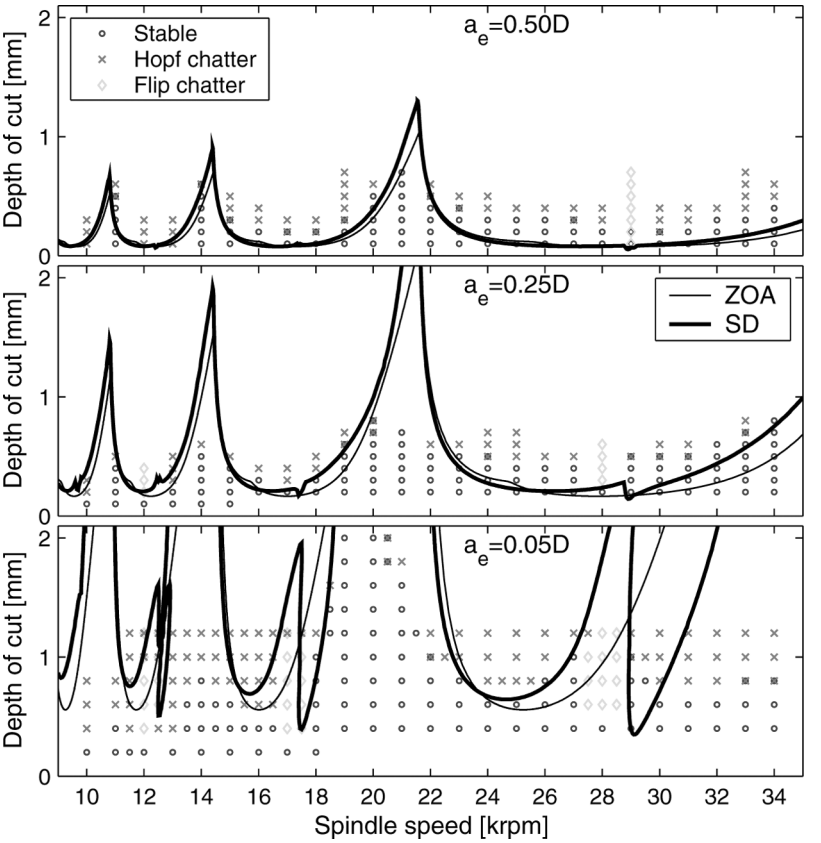

FIGURE 3 Comparison of experimental and predicted stability charts.

in the cutting tests: periodic chatter-free regime, quasiperiodic, and periodic chatter regimes. Figure 4 shows typical examples of the recorded tool motion in the X-Y plane, Y-displacement sampled exactly once per tooth passing period T, and the amplitude spectra of the Y-displacement for the three cases. In the chatter-free motion, the tool oscillates periodically with the tooth passing frequency Nn, which is in our case ($N = 1$) equal to the spindle speed n. This is confirmed by the $1/T$ sampled displacement where the data points are gathered in one compact cloud (panel (1a) in Figure 4) and their values remain approximately constant as cutting progresses (panel (1b)). The amplitude spectrum of the displacement shows peaks only at the multiples of the spindle speed (panel (1c)).

In quasiperiodic chatter, the tool moves on a torus defined by the dominant eigenfrequency and the tooth passing frequency, which usually have incommensurate values. The data points sampled once per tooth passing period lie on a circle (panel (2a)) and their values oscillate periodically

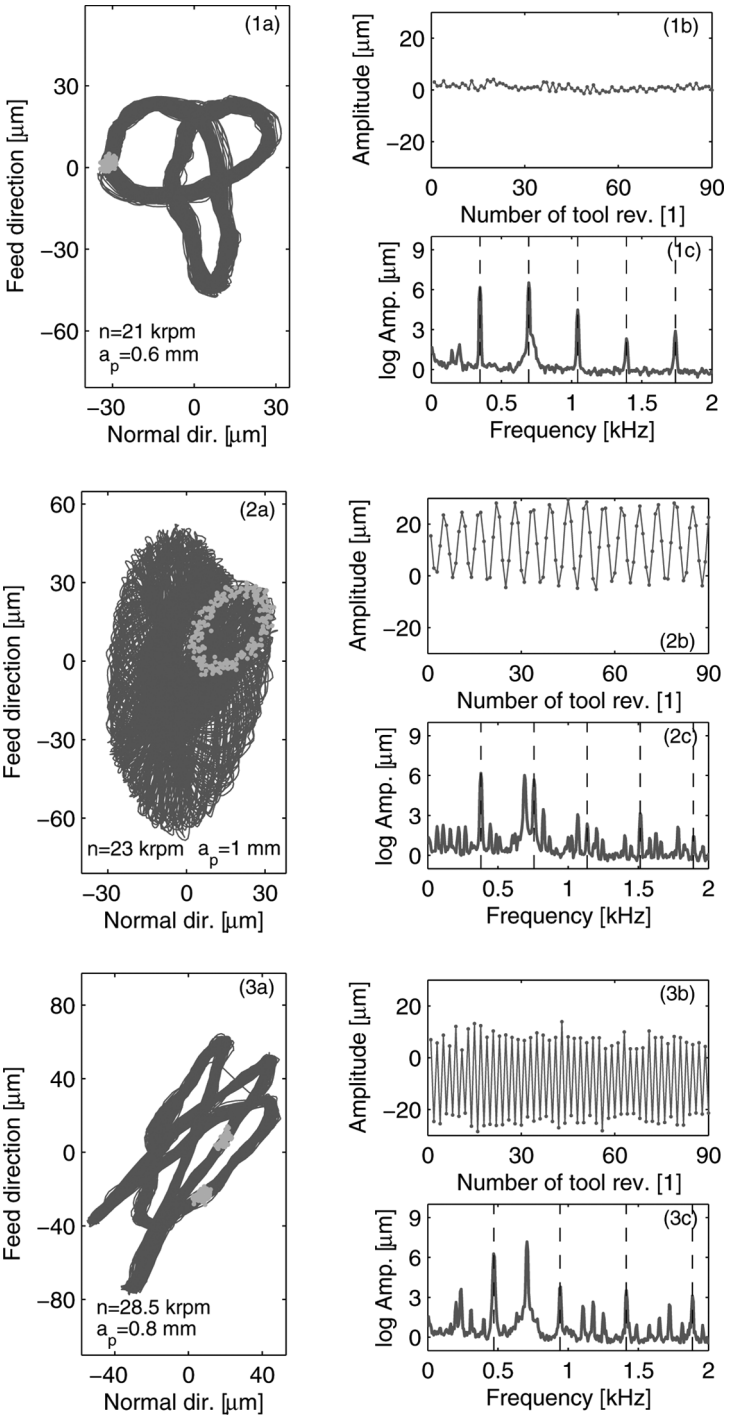

FIGURE 4 (∼a) Tool motion in X-Y plane, light dots denote $1/T$ sampled data, (∼b) $1/T$ sampled Y-displacement, (∼c) amplitude spectra of Y-displacement, vertical dashed lines denote multiples of the tooth passing frequency. (1∼) chatter-free, (2∼) quasiperiodic chatter, (3∼) period doubling chatter. All cases: $a_e = 0.05D$, up-milling.

in time (panel (2b)). Spectral peaks are found at the two frequencies, at their sums and differences and their multiples (panel (2c)).

Tool motion in periodic chatter is periodic with twice the tooth passing period, $2T$, (and half the tooth passing frequency, $Nn/2$). $1/T$ sampled data points form two compact clouds (panel (3a)), which are visited alternately (panel (3b)). The amplitude spectrum of the displacements shows peaks at the multiples of half the tooth passing frequency (panel (3c)). Note that chatter-free motion is also periodic but with a tooth passing period T. The difference between the periodic chatter-free and periodic chatter tool motion is therefore in the period. The chatter-free tool motion repeats itself after each tooth pass (period equals T), while the periodic chatter tool motion repeats itself after two tooth passes (period equals $2T$).

CONCLUSIONS

Stability boundaries predicted by the widely used zeroth-order approximation (ZOA) method and the recently proposed semi-discretization (SD) method were compared. Under the specified cutting parameters and the machine tool modal properties, the methods yielded similar predictions for high radial immersions. As radial immersion was decreased, the disagreement between the predictions of the two methods grew. For very low radial immersions, the predicted stability boundaries differed considerably. The most prominent difference was an additional set of lobes corresponding to the new type of instability, the period doubling bifurcation, which was predicted only by the SD method. Period doubling bifurcation causes periodic chatter as opposed to the quasiperiodic chatter caused by the Hopf bifurcation.

Experimental verification of the stability boundaries confirmed that the predictions of the SD were more accurate than those of the ZOA method, although both methods significantly overestimated the stability maxima at low immersions. All three different types of the tool motion predicted by the SD method were observed experimentally: periodic chatter-free, quasiperiodic, and periodic chatter. These types of tool motion were studied in more detail based on recorded tool deflections in the X-Y plane.

In summary, the presented investigations showed that there are indeed two types of instability possible in low radial immersion milling and both of them should be taken into account when selecting the stable, chatter-free cutting parameters.

ACKNOWLEDGMENTS

JG gratefully acknowledges support of the Alexander von Humboldt Foundation from Germany. TI was supported by the Magyary Zoltán

Postdoctoral Fellowship of Foundation for Hungarian Higher Education and Research, and together with GS, also by the Hungarian National Science Foundation under grant no. OTKA T043368.

REFERENCES

[1] Tlusty, J. and Poláček, M. (1963) The Stability of Machine-Tool Against Self-Excited Vibration in Machining, *Proceedings International Research in Production Engineering*. ASME, Pittsburgh, Pennsylvania, USA.

[2] Tobias, S.A. (1965) *Machine Tool Vibration*. Blackie & Son, Ltd., Glasgow, UK.

[3] Budak, E. and Altintaş, Y. (1998) Analytical prediction of chatter stability in milling–Part I: General formulation, *ASME Journal of Dynamic Systems, Measurement, and Control*, 120(1): 22–30.

[4] Budak, E. and Altintaş, Y. (1998) Analytical prediction of chatter stability in milling–Part II: Application of the general formulation to common milling systems, *ASME Journal of Dynamic Systems, Measurement, and Control*, 120(1): 31–36.

[5] Altintaş, Y. and Budak, E. (1995) Analytical prediction of stability lobes in milling, *Annals of the CIRP*, 49(1): 37–40.

[6] Davies, M.A., Pratt, J.R., Dutterrer, B., and Burns, T.J. (2000) The stability of low radial immersion milling, *Annals of the CIRP*, 49(1): 37–40.

[7] Insperger, T., Mann, B.P., Stépán, G., and Bayly, P.V. (2003) Stability of Up-Milling and Down-Milling, Part 1: Alternative Analytical Methods, *International Journal of Machine Tools and Manufacture*, 43(1): 25–34.

[8] Mann, B.P., Insperger, T., Bayly, P.V., and Stépán, G. (2003) Stability of Up-Milling and Down-Milling, Part 2: Experimental Verification, *International Journal of Machine Tools and Manufacture*, 43(1): 35–40.

[9] Mann, B.P., Young, K.A., Schmitz, T.L., Bartow, M.J., and Bayly, P.V. (2003) Machining Accuracy Due to Tool or Workpiece Vibrations. *Proceedings of IMECE'03*, ASME International Mechanical Engineering Congress 2003, Washington, DC, USA.

[10] Guckenheimer, J. and Holmes, P. (1983) *Nonlinear Oscillations, Dynamical Systems, and Bifurcations of Vector Fields*, Springer Verlag, New York.

[11] Gradišek, J., Kalveram, M., and Weinert, K. (2004) Mechanistic Identification of Specific Force Coefficients for a General End Mill, *International Journal of Machine Tools and Manufacture*, 44(4): 401–414.

[12] Szalai, R. and Stépán, G. (2003) Stability boundaries corresponding to period doubling are essentially closed curves. *Proceedings of* IMECE'03, ASME International Mechanical Engineering Congress, Washington, DC, USA.